Effect of the position and the number of broken bars in an Asynchronous Motor Stator Current Spectrum

A. Menacer*, S. Moreau**, A. Benakcha *, M. S. Naît Saïd ***

* LGEB. Electrical laboratory of Biskra, University of Biskra, B.p 145, 07000, Biskra, Algeria
menacer_arezki@hotmail.com
** LAII. Automatic and industrial informatics laboratory Pineau *avenue,40 Poitiers, 86 022 Cedex France*
*** LSPIE. Laboratory, University of Batna, Med El Hadi Boukhlouf Street 05000 Batna, Algeria

Abstract— **The asynchronous motor has an interest in applications of strong powers requiring the variation speed. However, it is not, like any other electric machine, safe from a dysfunction in consequence of failure of an electrical or mechanical nature.**

Among these rotor defects, we can quote a fissure or a total break of bar, a rupture of end ring circuit, an eccentricity of the rotor axis...

In this paper, we use a technique based on the spectral analysis of stator current in order to detect a break down or a defect in the rotor. Thus, the number and the position effect of the breaks has been highlighted.

The effect is highlighted by considering the machine supplied directly through a balanced three-phase network.

Index Terms- broken rotor bar, asynchronous motor, modeling, diagnostic, broken bars position, stator current.

I. INTRODUCTION

Although the asynchronous machine is famous for its qualities of robustness and its low cost of construction, it happens nevertheless that it can present electrical or mechanical failures types.

The developed signatures techniques analysis of the rotor defects (partial or total break in the squirrel-cage bar, portion of end ring) and of the stator defects (unbalance in amplitude or phase between stator phases) must allow to prevent a defect. From the analysis of this defect, we can program the stop of production process line for the failing elements replacement.

The early diagnosis and the detection of defects are of importance and raise difficulties to mobilize the researchers in the electrical engineering, automatic and signal processing fields.

Among the defects to be detected, we can quote the break bars and a portion of end ring on which any direct measurement is difficult.

The consequences of this defects type induce:

- a mechanical ageing of the rotor axis because of the torque fluctuations,
- higher risks of the adjacent bars break which carry high currents and, consequently, significant electrodynamics constraints,
- an influence on the machine supply signals shapes, therefore on the electric network.

We can also quote other defects types:

A.   Internal defects

The source of these defects is the behaviour of the machine.

STATOR DEFECTS

The stator is rather subjected to electric stresses which can be accompanied by the following defects:

- short circuit in the whorls of the same phase,
- short circuit between phases,
- cut in the phase,
- defect in the magnetic circuit (sheet rupture),
- defect in the sheet insulation,
- electric defect of insulation in the stator winding,
- following an ageing of insulators.

ROTOR DEFECTS

Among these defects we can quote:

- misalignment of the rotor in consequence of a wear of the bearings detectable by the monitoring of the vibrations or the current [1],
- break of one or several bars,
- break of end rings,
- defect of the magnetic circuit.

B.   External Defects

These defects must mainly with a problem of different nature:
- electrical: transitory mode or unbalance of the feeding,
- thermals: operating temperature raised, points hot, overload,
- mechanical: frictions, shocks in service,…
- chemical: corrosion, moisture.

In particular, outgoing research work is being concentrated on rotor bar faults and on the development of diagnostic techniques for three-phase squirrel-cage induction machines [2]–[4].

II. MODEL OF THE THREE-PHASE ASYNCHRONOUS MACHINE

The machine model development takes into account the following assumptions [5]:

- the saturation and the skin effect are negligible,
- the air-gap is uniform,
- the mmf distribution in the air-gap is sinusoidal,
- the rotor bars are isolated from the magnetic circuit of the rotor,
- the relative permeability of the machine magnetic circuit is supposed to be infinite.

Although the mmf of the stator winding is supposed to be sinusoidal, other distributions of rolling up could also be considered by simply employing the theorem of superposition. This is justified by the fact that the various components of the harmonics of space do not act the ones on the others [6]

In order to study the phenomena taking place in the rotor, this phenomena is currently modeled in the form of NR meshes as shown in figure 1.
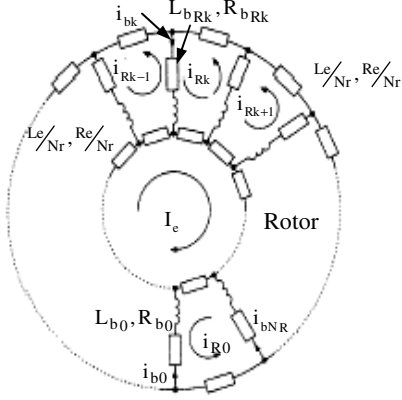

Figure 1. Rotor cage equivalent circuit

The induction motor mathematical model can be written as follows:

$$[V]=[R][I]+\frac{d}{dt}([L].[I]) \qquad (1)$$

with:

$$[V]=\begin{bmatrix}[V_S]\\[V_R]\end{bmatrix}, \quad [I]=\begin{bmatrix}[I_S]\\[I_R]\end{bmatrix}$$

and:

$$[V_S]=[V_{S1} \ V_{S2} \ V_{S3}]^t, \quad [V_R]=[0 \ 0 \ 0 \ \cdots \ 0]^t_{1\times(N_R+1)}$$

$$[I_S]=[I_{S1} \ I_{S2} \ I_{S3}]^t,$$

$$[I_R]=[I_{R1} \ .. \ I_{Rk} \ .. \ I_{RN_R} \ I_e]^t_{1\times(N_R+1)}$$

The resistance global matrix can be written as:

$$[R]=\begin{bmatrix}
[R_S]_{3\times3} & \vdots & [0]_{3\times N_R} & \vdots & [0]_{3\times1}\\
\cdots & \cdots & \cdots & \cdots & \cdots\\
[0]_{N_R\times3} & \vdots & [R_R]_{N_R\times N_R} & \vdots & -\frac{R_e}{N_R}[1]_{N_R\times1}\\
\cdots & \cdots & \cdots & \cdots & \cdots\\
[0]_{1\times3} & \vdots & -\frac{R_e}{N_R}[1]_{1\times N_R} & \vdots & R_e[1]_{1\times1}
\end{bmatrix} \quad (2)$$

where:

$$[R_S]_{3\times3}=\begin{bmatrix}R_S & 0 & 0\\ 0 & R_S & 0\\ 0 & 0 & R_S\end{bmatrix}$$

The inductance global matrix can be represented by:

$$[L]=\begin{bmatrix}
[L_S]_{3\times3} & \vdots & [M_{SR}]_{3\times N_R} & \vdots & [0]_{3\times1}\\
\cdots & \cdots & \cdots & \cdots & \cdots\\
[M_{RS}]_{N_R\times3} & \vdots & [L_R]_{N_R\times N_R} & \vdots & -\frac{L_e}{N_R}[1]_{N_R\times1}\\
\cdots & \cdots & \cdots & \cdots & \cdots\\
[0]_{1\times3} & \vdots & -\frac{L_e}{N_R}[1]_{1\times N_R} & \vdots & L_e[1]_{1\times1}
\end{bmatrix} \quad (3)$$

where:

$$[M_{SR}]_{3\times N_R}=\begin{bmatrix}
\cdots & -M_{SR}\cos(\theta+k.a) & \cdots\\
\cdots & -M_{SR}\cos(\theta+k.a-\frac{2\pi}{3}) & \cdots\\
\cdots & -M_{SR}\cos(\theta+k.a-\frac{4\pi}{3}) & \cdots
\end{bmatrix}, \quad \begin{array}{l}k=0,N_R-1\\[4pt] a=p\frac{2pi}{NR}\end{array}$$

$$[L_S]_{3\times3}=\begin{bmatrix}L_{Sp} & M_S & M_S\\ M_S & L_{Sp} & M_S\\ M_S & M_S & L_{Sp}\end{bmatrix}$$

The detailed expressions of $[R_R]_{N_R\times N_R}$ and $[L_R]_{N_R\times N_R}$ are respectively:

$$[R_R]_{N_R\times N_R}=\begin{bmatrix}
R_{b0}+R_{b(N_R-1)}+2\frac{R_e}{N_R} & -R_{b0} & 0 & \cdots & \cdots & \cdots & -R_{b(N_R-1)}\\
0 & \cdots & -R_{b(k-1)} & R_{bk}+R_{b(k-1)}+2\frac{R_e}{N_R} & -R_{bk} & 0 & \cdots & 0\\
-R_{b(N_R-1)} & 0 & \cdots & \cdots & 0 & -R_{b(N_R-2)} & R_{b(N_R-1)}+R_{b(N_R-2)}+2\frac{R_e}{N_R}
\end{bmatrix}$$

$$[L_R]_{N_R \times N_R} = \begin{bmatrix} L_{Rp}+2L_b+2\dfrac{Le}{N_R} & M_{RR}-L_b & M_{RR} & M_{RR} & \cdots & M_{RR}-L_b \\ M_{RR}-L_b & L_{Rp}+2L_b+2\dfrac{Le}{N_R} & M_{RR}-L_b & M_{RR} & M_{RR} & \cdots \\ M_{RR} & M_{RR}-L_b & L_{Rp}+2L_b+2\dfrac{Le}{N_R} & M_{RR}-L_b & M_{RR} & \cdots \\ M_{RR} & \vdots & \ddots & \ddots & \ddots & \ddots \\ \vdots & \ddots & \ddots & \ddots & \ddots & \ddots \\ M_{RR}-L_b & M_{RR} & M_{RR} & \cdots & M_{RR}-L_b & L_{Rp}+2L_b+2\dfrac{Le}{N_R} \end{bmatrix}$$

III. DEFECT MODEL OF THE MOTOR

In order to simulate the defect of bar break, we add to the corresponding element of the rotor resistance matrix R_R the defect resistance R_{bf} [7], such as:

$$[R_F]_{N_R \times N_R} = \begin{bmatrix} 0 & \cdots & 0 & \cdots & \cdots & 0 \\ \vdots & \cdots & \vdots & \vdots & \cdots & \vdots \\ \vdots & \cdots & 0 & 0 & \cdots & 0 \\ 0 & 0 & R_{bF_k} & -R_{bF_k} & 0 & 0 \\ 0 & 0 & -R_{bF_k} & R_{bF_k} & 0 & 0 \\ \vdots & \vdots & 0 & 0 & \vdots & \vdots \\ \vdots & \vdots & \vdots & \vdots & \vdots & \vdots \end{bmatrix}$$

Consequently, the squirrel cage resistance matrix, taking into account the defect, is defined by:

$$[R_{RF}]_{N_R \times N_R} = [R_R]_{N_R \times N_R} + [R_F]_{N_R \times N_R}$$

The mechanical equations must also considered:

$$\frac{d}{dt}\omega = \frac{1}{J_m}(Ce-Cr) \qquad (4)$$

with: $$\omega = \frac{d\theta}{dt}$$

and

$$Ce = \sqrt{\frac{3}{2}}\, p\, M_{SR}\left\{ I_{qS}\sum_{k=0}^{N_R-1} I_{R_{k+1}}\cos(k.a) - I_{ds}\sum_{k=0}^{N_R-1} I_{R_{k+1}}\sin(k.a) \right\} \qquad (5)$$

The application of the Park transform to the stator current and the use of mechanical equations allow to calculate stator currents.

IV. RESULTS AND DISCUSSIONS SIMULATION

After several transformations, the simulation of the machine is given by expressions (1) and (5).

The classical frequency domain analysis as the fast Fourier transform (FFT) is often used to detect frequency signatures by using a current probe on one of the machine stator phase [8]

The spectral analysis of the stator current highlights the effect of the defect which results in the appearance of the harmonics around the fundamental [9]-[11]

Their amplitudes increase according to the number of defective bars at characteristic frequencies (relation (6)), [12, 13].

$$f_{defect} = (1 \pm 2.n.g)fs, \qquad n=1,2,.. \qquad (6)$$

where f_{defect} are the sideband frequencies associated with the broken rotor bar, and g is the per-unit motor slip.

A. Effect of the break severity on the stator current spectrum

To highlight the effect of the break severity, we simulate bars break by increasing the broken bar resistance at 10 R_b and at 100 R_b.
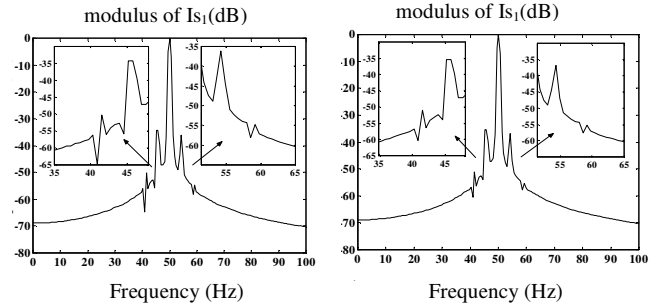

Figure 2. Stator current spectrum analysis when we have an increase of the broken bar resistance
a)10 Rb   b)100 Rb

It is noticed that the value of the broken bar resistance introduce a modification on the stator current spectrum (harmonics located on both sides the fundamental one), (figures 2-a and 2-b).

B. Effect of the number and the position of broken bars

We consider the break bars defect so that it is taken into account the number and the position of broken bars.
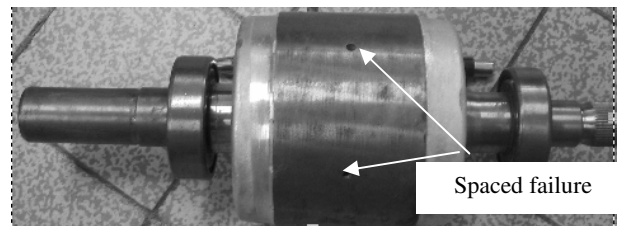

Spaced failure

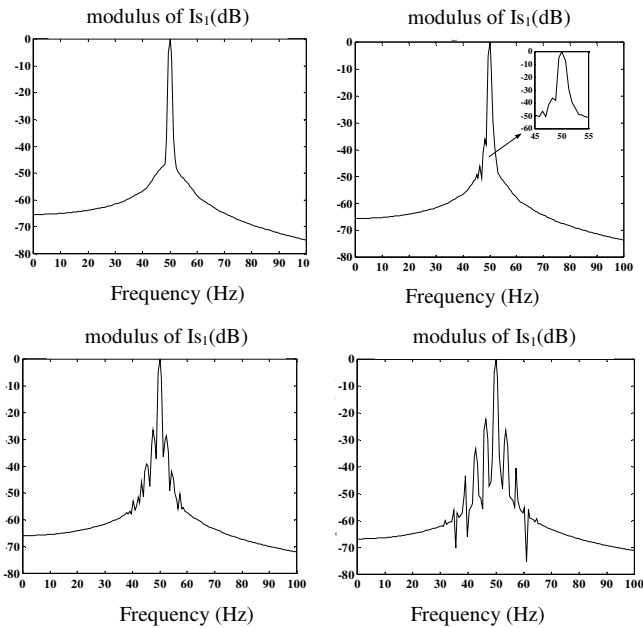Figure 3. Example of spaced broken bars

modulus of Is₁(dB) — various plots

Figure 4. Stator current spectrum with different slips for adjacent three break bars (g= 0.001%, g=1.15%, g=2.3 % and g=3.6 %)

On the figure (4), we notice the appearance of harmonics on the spectrum. These harmonics have amplitude which increases according to the raise in a number of defective bars and their positions. Table 1 highlights the influence of the number and the position broken bar spectrum.

The frequencies values given by the expression (6) and those deduced from the spectrum graphs are in agreement for various types of breaks [14]. The 3ed and 4th harmonic do not appear on the spectrum because there is compensation due to the relative position of the broken bars (cylindrical symmetry).

The increase in the harmonics amplitude is due to the increase in the number of broken bars.

The amplitude of the lines increases with the number of broken adjacent bars. In addition, the six lines corresponding to the defect appear.

C. Effect of the load on the stator current spectrum

The effect of the load (slip) on the stator current spectrum is highlighted by considering a break of three adjacent bars with different slips (g= 0.001 %, g=1.15 %, g=2.3 % and g=3.6 %).figure (5).

We notice a tightening of harmonics spectrum for the weak slips. The spectral analysis of signals becomes then delicate.

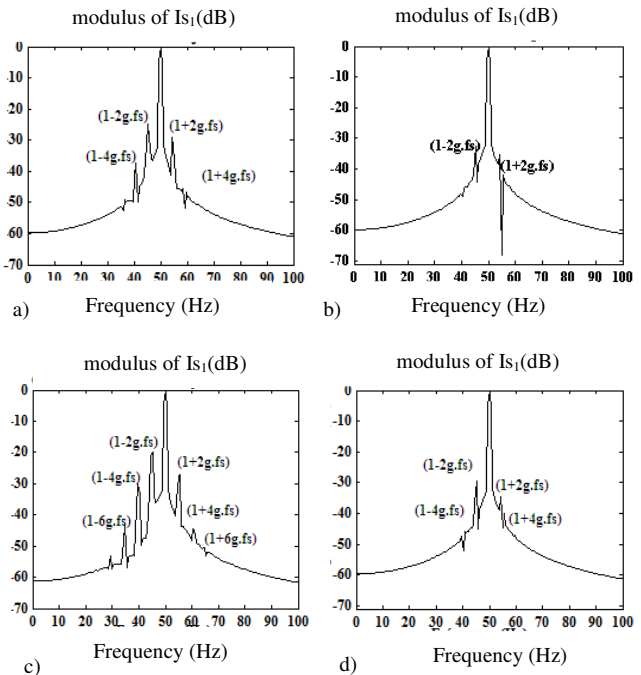

Figure 5. Stator current spectrum taking account of the number and the position of the broken bars   (g=3.6%)
a) adjacent two break bars   b) Spaced two break bars
c) adjacent three break bars   d) Spaced three break bars

In addition, it arises from figure. 5 that the defect is better highlighted when the machine is charged.

The number and the position of broken bars		$f_{cal}=(1-6g)fs$ raie 1	$f_{cal}=(1-4g)fs$ raie 2	$f_{cal}=(1-2g)fs$ raie 3	$f_{cal}=(1+2g)fs$ raie 4	$f_{cal}=(1+4g)fs$ raie 5	$f_{cal}=(1+6g)fs$ raie 6
a)	$f_{calculated}$ (Hz)	35.94	40.62	45.31	54.68	59.37	64.05
	$f_{deduced}$ (Hz)	36.58	40.87	45.11	54.33	58.57	63.54
	Magnitude (dB)	-49.16	-37.60	-24.91	-29.31	-45.6	-50.9
b)	$f_{calculated}$ (Hz)	36.26	40.84	45.42	54.57	59.15	63.73
	$f_{deduced}$ (Hz)	/	39.64	45.12	54.27	/	/
	Magnitude (dB)	/	-48.36	-32.71	-35.40	/	/
c)	$f_{calculated}$ (Hz)	34.576	39.71	44.85	55.14	60.28	65.42
	$f_{deduced}$ (Hz)	34.774	39.67	45.09	55.47	60.40	64.72
	Magnitude (dB)	-43.479	-30.46	-20.08	-27.00	-44.65	-50.81
d)	$f_{calculated}$ (Hz)	35.636	40.42	45.21	54.78	59.57	64.36
	$f_{deduced}$ (Hz)	/	40.83	45.137	54.15	59.79	/

Tableau 1. Frequencies and magnitudes of the stator current spectrum:
a) adjacent two break bars   b) spaced two break bars   c) adjacent three break bars   d) spaced three break bars

D. *Effect of broken bars position for the current spectrum*

In these cases, we consider two broken bars, the fault of broken bars as function of the angle position between two broken bars.
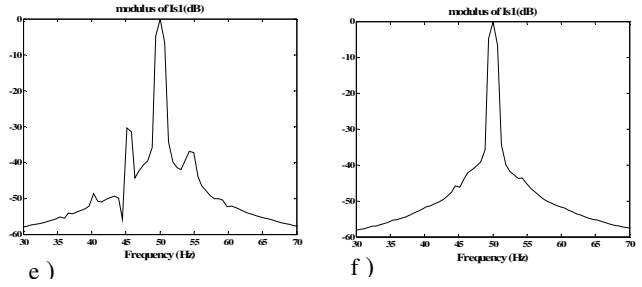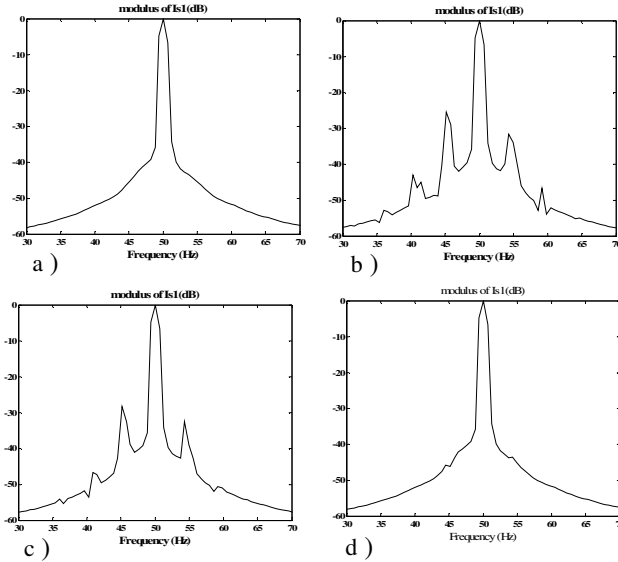

e)   f)

Figure 6.   Stator current spectrum with different position broken bars
a) healthy motor   b) α =22,5°   c)   α =45°
d) α =90°   e) α =135°   f)   α =180°

If the breaks of bars are near (figure 6b, 6c), the amplitude both sides of the fundamental harmonic are significant tableau 2. On the other hand if the position is with 90° or diametrically opposite (figure 6d, 6f), the amplitude of the raise is weak then it difficult is distinguished compared to the healthy machine (figure 6a).

a)   b)

c)   d)

		$\alpha = 22.5°$	$\alpha = 45°$	$\alpha = 90°$	$\alpha = 135°$	$\alpha = 180°$
Lower	f (Hz)	54.2857	54.2857	54.2857	54.2857	54.2857
		59.1705	59.1705	/	58.9862	/
		64.6083	/	/	/	/
	Magnitude (dB)	-31.6228	-32.4196	-43.5965	-36.8860	-43.5380
		-46.7325	-50.6360	/	-50.2193	/
		-55.0658	/	/		/
Upper	f (Hz)	45.1613	45.1613	44.5161	45.2535	44.6083
		40.2765	40.9217	/	40.2765	/
		36.0369	36.1290	/	36.4977	/
	Magnitude (dB)	-25.8699	-28.2237	-45.9357	-30.4825	-45.8772
		-43.0629	-46.8494	/	-48.9035	/
		-52.5804	-54.1155	/	-54.0789	/

Tableau 2. Effect of broken bars position for the current spectrum

Conclusion

This paper presents, within the framework of the diagnosis, the asynchronous motor broken bars simulation based on the development of a multi windings model.

The stator current spectrum analysis shows the presence of a defect due to the break or the rupture of bars at the frequencies given by the expression (6).

The severity of the defect results in the harmonics amplitude variation located on both sides of the fundamental harmonic.

Broken bar position and number effect result in increase of harmonics amplitude according to the number of broken bars. The defect of break in the adjacent bars is felt well in the spectrum. When the position of broken bars is 90° or 180°, the spectrum current analysis not distingue from the from the healthy

The effect of the load for:

- a weak slip (g) results in a contracting of the interval of harmonics,

- g significant (full load), the interval of harmonics widens and the amplitude increase.

The severity degree defect can be deduced from the amplitude of harmonics.

Generally, we noticed that the effect in the spectrum is of more much less visible than when the distance between two breaks is large.

The interval between these harmonics becomes broader, when the machine is with full load. At the broken bar, the variation of the slip can induce in error because it causes the appearance of additional harmonics (figure 4).

We can note that the slip is a significant parameter to take into account in the formulation of the diagnosis.

Pn	output power	1.1 kW
Vs	stator voltage per phase	220 V
fs	stator frequency	50 Hz
p	poles pair number	1
R_S	stator resistance	7.58 Ω
R_{b0}	rotor bar resistance	0.15mΩ
R_e	resistance of end ring segment	0.15mΩ
L_{b0}	rotor bar inductance	0.1μH
L_e	inductance of end ring	0.1μH
L_{sf}	leakage inductance of stator	0.0265H
M_{sr}	mutual inductance stator rotor	46.422mH
N_R	number of rotor bars	16
N_S	number of turns per stator phase	160
J_m	inertia moment	$0.0054 \, Nms^2$
Rb_{FK}	additional resistance of a defect rotor bar	
a	electrical angle of two rotor adjacent meshs	0.392
θ	angle between stator phase 1 and od axis	
g	slip	
f cal	frequencies calculated	
id_s, iq_s	Park's currents	
α	angle position between two broken bars.	

REFERENCES

[1]   William R. Finlley, Mark M. Hodowanec, "An analytical approach to resolving motor vibration problem", *IEEE* 1999, p. 217-232.

[2]   N. M. Elkasabgy and A. R. Easthem, "Detection of broken bars in the cage rotor on an induction machine," *IEEE Trans. Ind. Applicat.*, vol. 28, pp. 165–171, Jan./Feb. 1992.

[3]   ] M. E. H. Benbouzid, "Bibliography on induction motors faults detection and diagnosis," *IEEE Trans. Energy Conversion*, vol. 14, pp. 1065–1074, Dec. 1999.

[4]   D. Kostic-Perovic, M. Arkan, and P. Unsworth, "Induction motor fault detection by space vector angular fluctuation," in *Conf. Rec. IEEE-IAS Annu. Meeting*, vol. 1, 2000, pp. 388–394.

[5]   H. Razik, H. Henao and R. Carlson, " The Effect of Inter -bar Currents on the Diagnostic of the Induction Motor", 2004 IEEE pp 797-802

[6]   A. R. T. A. Lipo , "Complex vector model of the squirrel-cage induction machine including instantaneous rotor bar currents" , *IEEE Transaction on Industry Application*, Vol.35,   N06, Nov/Dec 1999.

[7]   A. Abed, L. Baghli, H.Razik, A. Rezzoug , "Modeling induction motors for diagnosis purposes", *EPE' 99 Lausanne.*

[8]   M. Artioli, A. Yazidi, F. Filippetti, G.A. Capolino, "A general purpose software for signal processing oriented to the diagnosis of electrical machines," Proceedings of IEEE International Symposium on Industrial Electronics Conference *(ISIE'04)*, Ajaccio (France), May 2004, vol. 2, pp.809-814.

[9]   A. Menacer, M. S. Nait Said, A. Benakcha, S. Drid, "Stator current analysis of incipient fault into asynchronous motor rotor bars using Fourier   fast transform", *Journal of* Electrical *Engineering, Slovakia*, Vol. 5-6, 2004,pp 122-130

[10] A. Menacer, M. S. Nait Said, A. Benakcha, S. Drid, "Détection d'une Cassure de Barre Rotorique d' un Moteur Asynchrone par Analyse Spectrale du Courant Statorique", *CNGE'2004, première Conference nationale sur le génie électrique* 29/11/-01/12 2004 , pp 261-265, université Ibn Khaldoun Tiaret – Algérie

[11] A. Abed, L., E. Weinachter, A.Razik, A. Rezzoug ,"Real time implementation of the Sliding DFT Applied to on line's broken bars diagnostic", *IEEE International Electric machines and drives Conference, IEMDC'2001, Cambridge, MA USA,* June17, 20, 2001, p. 345-34

[12] M Benbouzid, "A Review of induction motors signature analysis as a medium for fault detection", *IECON'98, Aachen ,* Germany, 1998, pp 1950-1955

[13] Bulent Ayhan,, Mo-Yuen Chow, and Myung-Hyun Song, "Multiple Signature Processing-Based Fault Detection Schemes for Broken Rotor Bar in Induction Motors", IEEE TRANSACTIONS ON ENERGY CONVERSION, VOL. 20, NO. 2, JUNE 2005

[14] A. Menacer, M. S. Nait Said, A. Benakcha, S. Drid, "Stator Current Analysis of Incipient Fault into Induction Machine Rotor Bars", Journal of Electrical Engineering, Romanie, Vol 4 N°2– 2004, pp 5-12.